

# The Role of Ion Acoustic Instability in the Development of the Azimuthal Current Density Profile in Liner Experiments at 1 MA

Simon C. Bott-Suzuki<sup>1</sup>, *Member, IEEE*, Samuel W. Cordaro, L. Atoyán, *Graduate Student Member, IEEE*,  
T. Byvank<sup>2</sup>, *Graduate Student Member, IEEE*, W. Potter, B. R. Kusse, J. B. Greenly,  
D. A. Hammer, *Fellow, IEEE*, and C. A. Jennings

**Abstract**—Recent work reported on the current density in pulsed-power-driven liners where a vacuum gap was introduced in the power feed connecting the liner to the generator. The resultant gap flashover generates azimuthally localized current-carrying plasma channels, which can create an azimuthal nonuniformity in the current density. The current density evolves during the current pulse, but nonuniformity is observed through the experiment timescale. Magnetohydrodynamic simulation work in 3-D demonstrates the difficulty in reproducing the experimental data within a limited computational domain, and those boundary conditions may dominate this paper. The development of current-driven instabilities in the plasma channels can explain the liner current density evolution, and specifically the ion acoustic instability can account for the main features observed in the experiments.

**Index Terms**—Current density, plasma pinch, plasma stability, vacuum breakdown.

## I. INTRODUCTION

THE realization of high-gain inertial fusion and the development of fusion energy remain a significant goal, and challenge, for high-energy density research. In the Z-pinch community it is presently envisioned that the compression of magnetized solid liners filled with DT fuel combined with the development of modular linear transformer driver pulsed-power devices will provide a viable path to repetition-rated fusion yield [3], [4].

The Z-pinch target approach is termed as magnetized liner inertial fusion (MagLIF), and was described by Sutz *et al.* [5] in 2010. The liner is an aluminum or beryllium cylinder, typically  $\sim 10$  mm tall,  $\sim 6$  mm in diameter with a wall thickness of order  $300 \mu\text{m}$ . Fuel is initially contained using

a thin-plastic window at the top of the liner, which also allows for laser preheat of the fuel. An external magnetic field of up to 30 T is applied and penetrates the target prior to the main current pulse. This field serves to both reduce heat loss through electron and alpha particle transport, and may help to stabilize the inner wall of the liner [6]. Radial compression of the liner is achieved using the 20-MA, 100-ns Z current pulse, and the fuel reaches ignition temperature at moderate convergence ratios. Although several areas require further study and optimization, recent fully integrated studies show a good reason for optimism at present [7], [8].

The work in this paper focuses on the initiation of plasma in the liner at the first application of the main drive current through experiments at the 1-MA, 100-ns Cornell Beam Research Accelerator (COBRA) generator at Cornell University [9]. Effective symmetric coupling of the liner to the pulsed-power generator is a crucial factor in the MagLIF scheme, since an azimuthally symmetric uniform compression of the liner is required, necessitating a uniform current drive throughout the target during the entire experiment. On the Z machine, various methods to mount the liner have been used. The liner target is typically fixed to the upper electrode (anode) and this assembly is inserted into the lower electrode (cathode) which is fixed into the generator. After insertion, there remains a small azimuthal gap between the liner and the cathode (i.e., a radial gap between coaxial electrodes which extends around the entire azimuth of the liner), which is of order  $25 \mu\text{m}$ . This is either left empty, so a vacuum gap is present for the experiment, or filled with epoxy or similar material. Studies to date have focused on the vacuum gap and its effect on plasma formation, demonstrating that even such a small gap can generate localized plasma which directly affects the current distribution in the liner, at least at the 1-MA level. While the research presented here is most pertinent for the MagLIF scheme, the initiation and current symmetry of Z-pinch and Z-pinch liners is important for the other fusion concepts and basic science and applied experiments

Here, we summarize the findings of the COBRA experiments, present magnetohydrodynamic simulation (MHD) work and a theoretical framework which accounts for the main features of the evolution of the azimuthal current density profile.

Manuscript received August 28, 2017; revised October 30, 2017; accepted December 2, 2017. This work was supported by the Center of Excellence in Pulsed Power High Energy Density Plasmas through the NNSA SSAA Program under DOE Cooperative Agreement DE-FC03-02NA00057. The review of this paper was arranged by Senior Editor S. J. Gitomer. (*Corresponding author: Simon C. Bott-Suzuki.*)

S. C. Bott-Suzuki and S. W. Cordaro are with the University of California, San Diego, La Jolla, CA 92093 USA (e-mail: sbottsuzuki@ucsd.edu).

L. Atoyán, T. Byvank, W. Potter, B. R. Kusse, J. B. Greenly, and D. A. Hammer are with Cornell University, Ithaca, NY 14850 USA.

C. A. Jennings is with the Sandia National Laboratories, Albuquerque, NM 87185 USA.

Color versions of one or more of the figures in this paper are available online at <http://ieeexplore.ieee.org>.

Digital Object Identifier 10.1109/TPS.2017.2783192

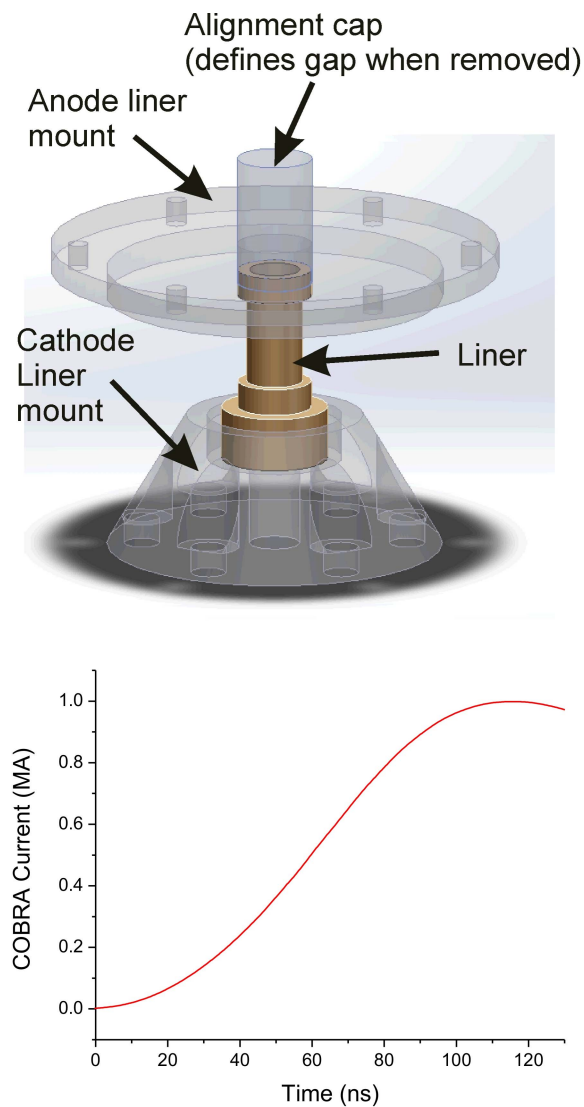


Fig. 1. Schematic of the liner mounting alignment and orientation for COBRA experiments, and typical drive current for the liner experiments.

## II. EXPERIMENTAL STUDIES

Experimental work studies a series of aluminum liners 6.3 mm in outer diameter and between 10 and 30 mm tall. Wall thicknesses are 300 and 150  $\mu\text{m}$ , both of which are large compared to the initial collisionless skin depth of  $\sim 20 \mu\text{m}$ . We do not use DT fuel in the liner, nor use an axial  $B$ -field for this paper. The presence of a uniform axial  $B$ -field may affect the plasma formation timescale, but is unlikely to influence the azimuthal asymmetries discussed in the following. The liners were mounted in the COBRA pulsed-power generator (100 ns, 1 MA). The lower connection to the power feed was fixed with conducting epoxy to ensure an excellent electrical contact. This used both a silver epoxy (cured conductivity  $7 \times 10^{-5} \Omega \cdot \text{m}$ ) to provide bulk adhesion and a silver conductive paint (cured conductivity  $2 \times 10^{-6} \Omega \cdot \text{m}$ ). The upper connection was configured to maintain a well-defined azimuthal gap to the upper electrode by using a tight-fitting alignment cap (Fig. 1). The wall thickness of the cap and the aperture in the upper electrode and gaps sizes of 200 and 400  $\mu\text{m}$  were

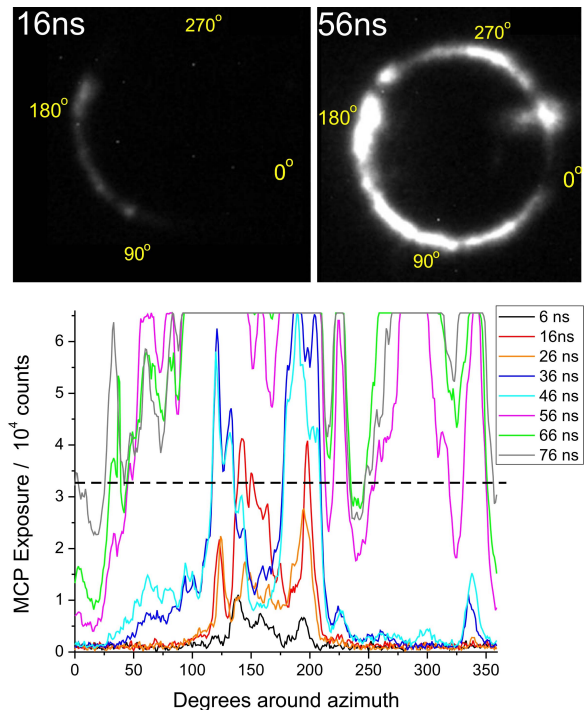


Fig. 2. Optical gated (10 ns) frames obtained at times indicated, along with azimuthal lineouts for several frames taken for a liner with a 400- $\mu\text{m}$  vacuum gap.

used in this paper. Tolerances give an estimated accuracy of the gap size and alignment of  $\sim 10 \mu\text{m}$ .

The primary diagnostics were a fast-framing optical camera (Invisible Vision UHSi 12/24), which provides up to 12 frames per experiment with frame exposures of 10 ns, laser gated imaging interferometry, and an array of magnetic field probes used to assess the azimuthal uniformity of the current density in the liner [10]. The optical framing camera was mounted to image the liner from above, giving a direct view of the vacuum gap around the liner throughout the experiment. The images obtained provide an excellent diagnosis of the plasma formation around the azimuth of the liner, and recent work directly linked the formation of emission regions in these images to the distribution of current density [2]. Here, we focus on the evolution of emission regions around the liner in an attempt to discern the driving mechanism for the evolution of the emission profile, and hence the azimuthal current density distribution.

An example of the evolution of emission is shown in Fig. 2 for an experiment using a 400- $\mu\text{m}$  vacuum gap around the liner. At early times, a low level of emission is observed in a localized region between approximately 100° and 200°. This region grows in intensity for the next several frames, before saturating the detector in the 56-ns frame. Notice that in the 36-ns frame, additional emission regions develop around 50° and also grow through the time sequence. Much of the azimuth shows little emission until relatively late in the current drive. The area at 340° shows no emission until 36 ns, and after this a localized emission spot grows over the next 30–40 ns, saturates the detector at  $\sim 66$  ns. The region between 250° and 300° is similarly dark until 46 ns, and then grows rapidly

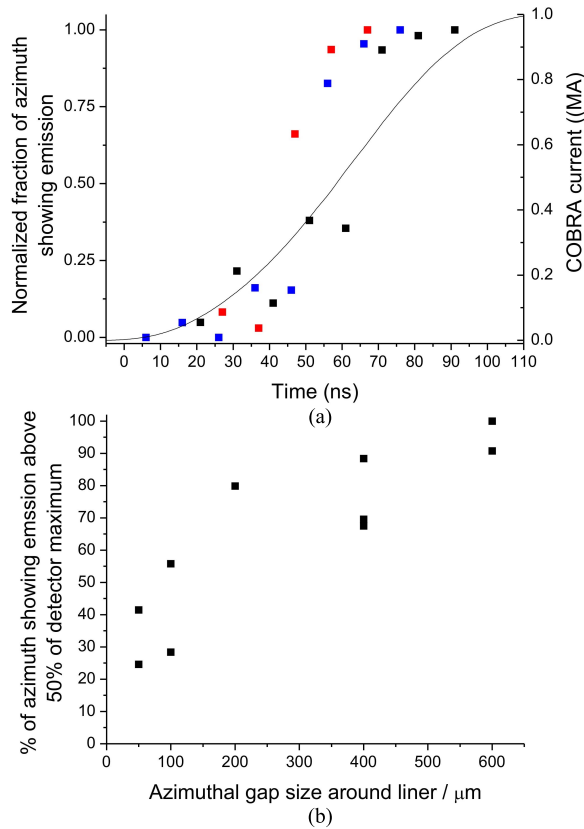


Fig. 3. (a) Plot of the fraction of azimuth showing emission above 50% saturation (see Fig. 2) overlaid on the COBRA current drive for 400- $\mu\text{m}$  gap shots (different colors are different shots). (b) Peak fraction observed against initial vacuum gap size.

in emission over just a single 10-ns interframe time. This sequence of small emission regions growing in intensity, along with new regions developing and also increasing in intensity is observed in all experiments. Typically, the fraction of the azimuth showing emission at late time is  $>25\%$ , but rarely is much greater than  $\sim 90\%$ . Images in which the entire azimuth showed uniform emission were not observed. Emission frames and streak images taken with a radial view of the liner showed the formation of surface plasma correlated with the azimuthal images [1], [2].

One way of quantifying this process is to examine the fraction of the azimuth which shows emission as function of time. To perform such an analysis, we need to select a suitable exposure level from the lineout plots, and we select 50% of the saturation level (dashed line in the plot in Fig. 2). This is somewhat arbitrary, but is a reasonable selection when comparing the resulting lineout to the optical images. Examination of 30% and 70% level generate similar results to those discussed in the following.

Fig. 3(a) shows both the evolution of the fraction of the azimuth showing emission and the current from the COBRA machine during the experiment. It can be seen that the evolution of the emission around the liner starts at a low level and grows relatively slowly for the first 50 ns. After this, the fraction appears to increase slightly more quickly until an upper limit is reached and no further fraction of

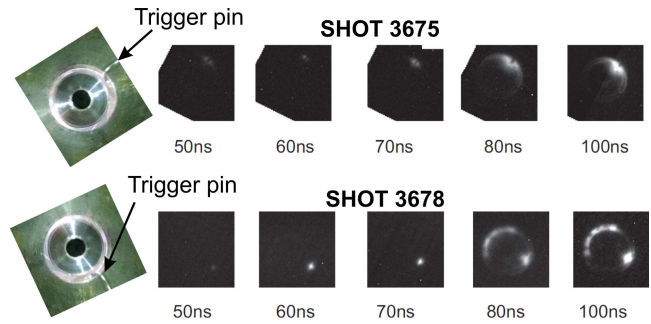


Fig. 4. Gated (10 ns) optical framing images of two nominally identical liner shots in which a trigger pin causes breakdown in a predetermined azimuthal position.

the azimuth develops emission regions. Note that the plot in Fig. 3(a) shows the fraction of the azimuth normalized to this peak value. It appears that the development of additional positions of emission around the azimuthal are related to the increasing current drive rather than, for example, early time voltage breakdown.

Fig. 3(b) shows the upper limit of the azimuth illuminated as a function of the gap sizes examined. In general, smaller gaps sizes show a smaller fraction of the azimuth in emission, and this increases as gap size increases. This trend is perhaps counterintuitive, since a smaller gap size leads to a higher electric field for the same applied voltages. The peak value of the fraction of the azimuth filled is likely a function of the exact plasma conditions at each location, and does not depend on the gap size. Examination of the evolution of the liner emission, and therefore azimuthal current density, suggests that this is not directly related to the initial voltage breakdown of the gap.

To examine this further, we carried out experiments in which the vacuum gap around the liner is encouraged to breakdown in one azimuthal position by using a “trigger pin.” This is a 100- $\mu\text{m}$  diameter wire inserted into the vacuum gap, and the initial position of emission is then determined by this pin. The results of six shots using this method showed two different trends, as shown in Fig. 4. In some shots (two of six shots, e.g., shot 3675), the initial pin position at which breakdown occurred dominated the emission profile, and little emission at additional azimuthal position was observed. In other shots (four of six shots, e.g., shot 3678), the initial breakdown position dominates only initially, after which other distinct emission regions develop. Previous work [2] again demonstrated that the current redistributes around the liner as the new positions emit.

The experimental data show an interesting set of trends, the interpretation of which is not straightforward. The key questions here are why do additional plasma channels form during the current drive, and what determines the rate at which they are generated. We attempt to address these issues through simulation and theoretical work in the following.

### III. SIMULATIONS

MHD simulation work has been carried out using the 3-D resistive MHD code Gorgon [11]. The modeling of the liners is a challenging task given the spatial scales involved.

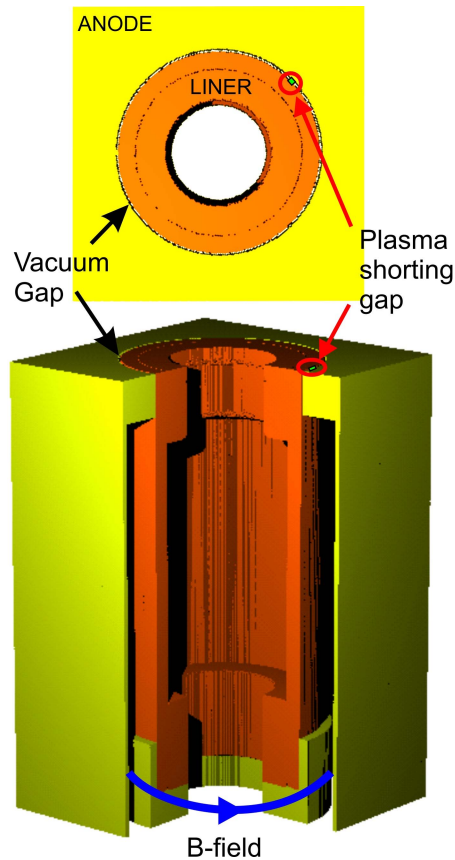


Fig. 5. Setup of Gorgon MHD simulations for liner shorted by plasma in one azimuthal position. Magnetic field boundary condition is applied at the lower boundary of the computational domain.

The liner is of centimeter scale, but the small vacuum gap must also be resolved. In addition, it is often useful to capture the electrode geometry to accurately describe current flow to and away from the load. The simulation presented here use a uniform  $20 \mu\text{m} \times 20 \mu\text{m} \times 20 \mu\text{m}$  cell size. A sample of the computational volume is given in Fig. 5. The domain contains a minimal portion of the electrodes, and the current is driven using a magnetic field boundary condition. This is applied to the lower boundary, away from the position of the vacuum gap shorted by the initial plasma. Since Gorgon is an MHD code, the breakdown phase, which is driven by electron and ion acceleration in the applied electric field at the vacuum gap, is not modeled. Instead, the initial conditions use a low density, low-temperature plasma at one azimuthal position across the vacuum gap. This is analogous to the “triggered” experimental shots discussed previously, and the primary interest is in the evolution of the current density in the liner after this time.

For simulations of azimuthal gaps of  $20 \mu\text{m}$ , there was no observable effect of this initial asymmetry on the liner implosion. Simulations using an exaggerated gap size of  $500 \mu\text{m}$  were subsequently carried out and are summarized in Fig. 6. The plasma short across the large vacuum gap is again in one azimuthal location and the plots shown are taken at a drive current of 1 MA on the Z machine, which is just as the main drive current is beginning. In this case, effect of

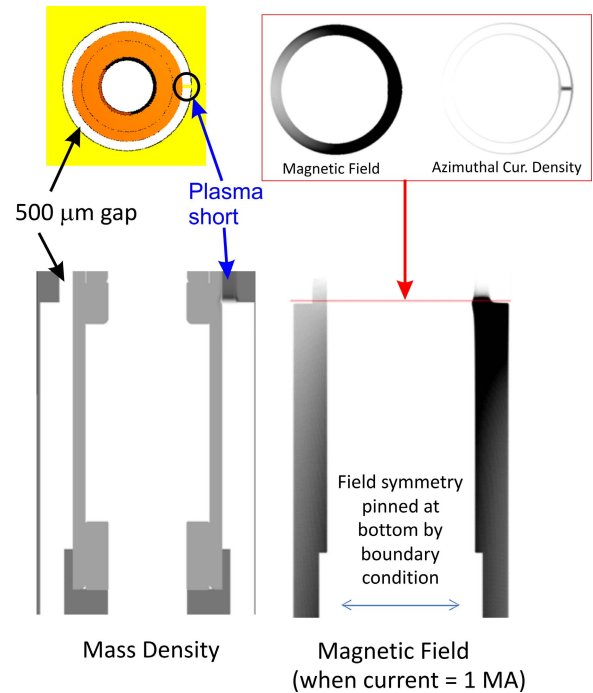


Fig. 6. 3-D Gorgon simulations of the evolution of the mass density of a liner on Z during an implosion when initiated with a  $500\text{-}\mu\text{m}$  vacuum gap closed at one azimuthal position. Azimuthal plots of magnetic field and current density (red box) are taken at the axial position indicated.

the initial asymmetry persists for a short period. There is a difference in the current density by a factor of  $\sim 20$  in the liner, where the initial plasma short is located compared to a position on the opposite side of the liner. This is reflected in a difference in the magnetic field around the liner at the same location (azimuthal plot in Fig. 6). The larger gap in this case breaks the feedback between the ablation of the electrodes and the symmetrizing of the current drive, because the large gap takes a finite time to close and allow this to occur. Note, however, that the lower portion of the liner shows uniform current density magnetic field, since this is dictated by the boundary conditions. As soon as the vacuum gap closes due to ablation, the liner implosion proceeds with a uniform azimuthal current, and the final stagnation is again uniform, as in the small gap case.

It is likely that the boundary conditions drive the current symmetry in these simulations. At the lower boundary, the condition for the  $B$ -field here is simply  $B = \mu_0 I / 2\pi r$ , which spatially depends only on the radius from the liner axis, and is therefore azimuthally symmetric. Since this must be met in the liner, even if the initial current is asymmetric (i.e., depends on both the radius and angle) it must return to the boundary condition set by the simulation. This is problematic in accurately reproducing the experimental observations. There are approaches that could be used to provide a more accurate description. The first is to significantly increase the size of the computational domain to allow the boundary condition to be set remotely from the liner. This involves including an increased portion of the power feed as well as the liner electrodes which must be treated accurately. In addition, as is

obvious from the nature of the experiment, this must be simulated in 3-D and so even small increases in the domain size infers a large increase in the volume modeled at the high-spatial resolution required to resolve the small vacuum gap. This process quickly becomes computationally prohibitive. An alternative is to modify the way in which the liner is attached to the generator power feed. The computational boundary could be linked to spatially distributed transmission line network that can support and evolve large current asymmetries. Each azimuthal section of such a power feed could support a current density essentially independent of its neighbor, again governed by a remote boundary condition. This approach may be promising, but requires significant development of the code and such a capability is not available at present.

The crucial contrast to the COBRA experiments is that the simulations show rapid azimuthal redistribution of the current density until this is uniform, whereas the experimental data show localized plasma locations around the azimuth which persist as seemingly discrete current channels. The conclusion here is that either the boundary conditions dominate any other effects or that the experiments are driven by non-MHD effects. In Section IV, we discuss a theoretical framework to address the main feature of the experiments.

#### IV. DISCUSSION

The primary features noted previously are the development of additional plasma channels, and the relatively slow timescales on which this occurs. Each of the channels continues to show emission after new ones are formed, suggesting current is flowing in some distribution across all the observed channels. There are several current-driven instabilities which may play a role in the experiments. In Z-pinch plasma experiments the most likely candidates are the lower hybrid and ion acoustic instabilities due to the plasma temperature and density ranges expected, as discussed in Ryutov *et al.* [12]. The effect of these instabilities in a current-carrying plasma is to introduce local density perturbations which significantly increase the scattering of electrons, thereby increasing the effective resistivity of the plasma. Other instabilities which can develop in such a plasma channel or column include the various MHD modes including the pinch  $m = 0$  mode, but most of these primarily affect the morphology leading to physical disruption or breakage of the channel. In this case, the current in an unstable channel would likely decrease if it is disrupted, accompanied by strong emission from a pinch or electron beam formation. Such features are not observed by XUV self-emission images or filtered X-ray diodes in our present experiments.

For this discussion, we consider the experimental data from the “triggered” shots, in which the vacuum gap is closed by plasma formation in one known azimuthal position. We assume an initial plasma channel has formed, similar to some experimental images (Fig. 7), and takes all the drive current. As shown in Fig. 4, identical shots can show either the formation of several subsequent plasma channels during the current drive or that no other channels form.

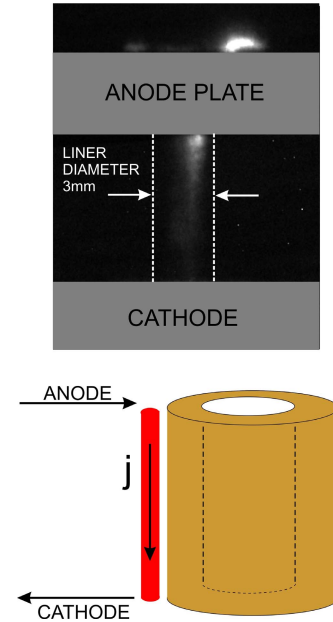


Fig. 7. Experimental gated (10 ns) optical emission of a liner showing localized plasma channel formed, and schematic representation of plasma channel formation at the liner surface.

From experimental data in [1] and [2], we can suggest reasonable estimates for the plasma channel parameters. Surface plasma is observed in some cases in interferometry images and only rarely in shadowgraphy images, suggesting that the plasma density is unlikely to be higher than  $n_e \sim 10^{19} \text{ cm}^{-3}$ . The emission from the surface plasma is observed in optical frames, but not in XUV frames, suggesting that the electron temperature is not higher than about 10 eV. We assume that the electron and ion temperature are the same  $T_e = T_i$  and estimate an upper ionization level for aluminum of  $Z \sim 8$  from the Thomas–Fermi model. The optical images give a typical plasma channel radius of  $\sim 0.5 \text{ mm}$ . While these are rather general estimates, and would be improved with additional data, they are consistent with experimental data and provide a good guide for the following discussion. From these values, we can estimate parameters such as the ion sound speed  $c_s$ , ion thermal velocity  $v_{ti}$ , cyclotron ( $\omega_{ce}$ ), and plasma ( $\omega_{pe}$ ) frequencies as required.

The electron drift velocity  $u_{\text{drift}}$  in a current-carrying plasma is determined from the current density  $j$  through  $j = n_e e u_{\text{drift}}$ , where  $n_e$  is the plasma density and  $e$  is the electronic charge. At high-current densities, the drift velocity can greatly exceed the sound speed which triggers instability growth for both the ion acoustic and lower hybrid modes. For the above parameters, at  $I = 95 \text{ kA}$  (20 ns into the COBRA current drive)  $u_{\text{drift}}$  is  $1.2 \times 10^5 \text{ m/s}$  and  $c_s = 2.5 \times 10^4 \text{ m/s}$ , and  $c_s > v_{ti}$  by about a factor of 5, meaning that ion motion cannot smooth out density perturbations driving the instability.

The lower hybrid instability has a simplified frequency given by  $\omega_{\text{LH}} = \omega_{ce} \sqrt{(Z m_e / A m_p)}$  (where  $Z$  is the ionization state,  $m_e$  is the electron mass,  $A$  is the atomic mass, and  $m_p$  is the proton mass) [11]. Throughout the experiment, this is always much less than the electron gyrofrequency

( $\omega_{LH} = 1.1 \times 10^{11} \text{ s}^{-1} \ll \omega_{ce} = 1 \times 10^{13} \text{ s}^{-1}$ ), so this cannot lead to an increase in plasma resistivity. In addition, the plasma frequency is much greater than the cyclotron frequency ( $\omega_{pe} = 2 \times 10^{14} \text{ s}^{-1} \gg \omega_{ce}$ ) leading to strong growth of the ion acoustic instability over the lower hybrid. In this case, the ion acoustic instability grows rapidly, resulting in a rapid increase in the plasma resistivity. The rapid turn ON of this process essentially limits the drift velocity to a value of  $u_{\text{drift,critical}}$  of a few times the ion sound speed. This in turn then limits the peak current density a plasma channel can carry, and therefore the absolute current for a given channel dimension [13]. Here, we take the value of the critical drift velocity to be  $u_{\text{drift,critical}} \sim 4c_s$ . The combination of an increase in resistivity and the resultant current limit for a plasma channel can explain the experimental behavior as we discuss in the following.

Starting from our simplified scenario in Fig. 7, we assume all the current is carried in the plasma channels at the liner surface. Assuming the plasma column dimensions, density and temperature change only slowly, the increasing current drive causes an increase in the electron drift velocity, triggering ion acoustic instability, and a rapid increase in resistivity. This has two principle effects. First, the resistance of the plasma column  $R = \rho/lA$  increases (where  $\rho$  is resistivity,  $l$  is the conductor length, and  $A$  is the cross-sectional area), and so the voltage drop across the electrodes increases. This is given by  $V = l \frac{dI}{dt} + L \cdot \frac{dI}{dt} + IR$ . The liner does not move during the experiments, and so the inductance remains fixed. This simplifies the voltage drop to  $V = L \cdot \frac{dI}{dt} + IR$ , and as the resistivity increases the latter term drives a large resistive voltage across the original azimuthal gap. This leads to an additional breakdown and plasma formation at another point on the liner, generating an additional plasma channel. The timing of this process is a result of the rapid turn of the ion acoustic instability. Once the electron drift velocity reaches its peak value of approximately 4 times the sound speed, this determines the peak current that can be carried by the original plasma channel. From the values above, this is  $I_{\text{channel,max}} \sim 150 \text{ kA}$ . Once the drive current reaches this, the resistive voltage rapidly increases causing a secondary gap breakdown. If the two plasma columns have similar parameters, at a drive current of 300 kA, the process repeats generating a third and then further plasma channels around the liner.

In Fig. 8, we show the number of channels formed as the current on COBRA increases using the above assumptions. For  $I_{\text{channel,max}} \sim 150 \text{ kA}$  the number of channels is relatively low. If the density is lower, assuming a similar temperature and spatial dimension, the maximum current is lower since there are less electrons to carry the current. Therefore, the velocity needs to increase to carry the required current, reaching the limit of  $4c_s$  more rapidly. The result is that if the original plasma channels are of lower density, there must be more of them to carry the total current at any given time in the COBRA experiments. Fig. 8(b) shows the number of channels formed for  $n_e = 1 \times 10^{19}$ ,  $5 \times 10^{18}$ , and  $1 \times 10^{18} \text{ cm}^{-3}$  assuming that all channels are identical.

For the lowest density, many channels are rapidly formed since each can only carry 15 kA each. Fig. 8(c) shows uses the

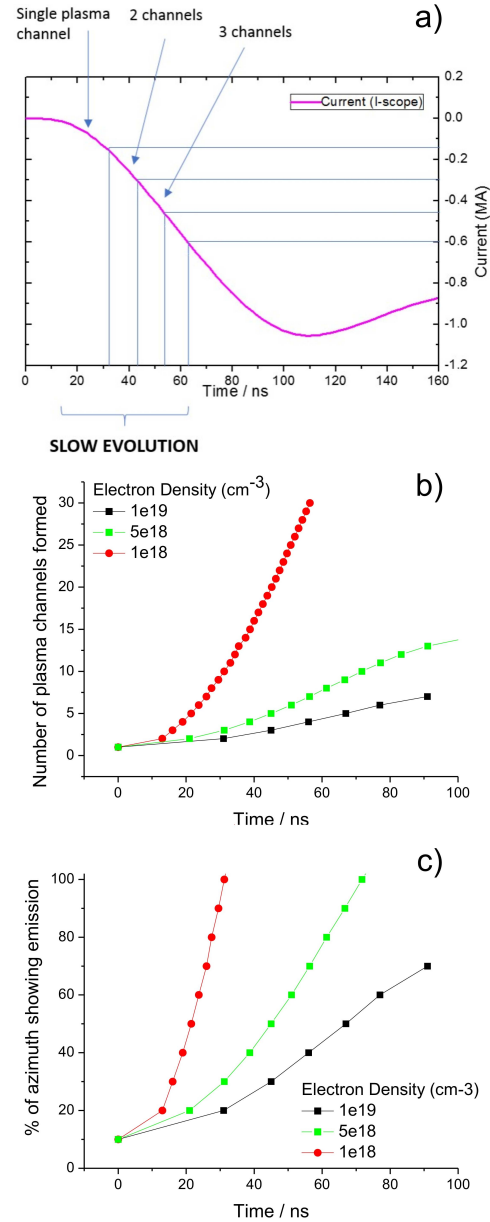


Fig. 8. Possible evolution of the number of channels based on resistivity increase due to the ion acoustic instability. a) Timing of the formation of plasma channels assuming  $I_{\text{channel,max}} = 150 \text{ kA}$  overlaid on the COBRA current drive. b) Number of plasma channels. c) Fraction of the azimuth showing emission with varying plasma electron density.

same data showing the fraction of the liner azimuth showing emission, and therefore carrying its local maximum current assuming a diameter of 0.5 mm for each channel. Although we cannot account easily for the detector saturation in the experiments, the general form of this plot is similar to that observed in the imaging lineouts in Fig. 3. Of course, the plasma channels are likely to be changing density and temperature throughout the experiments. The exhaustive analysis of the various parameters is beyond the scope of this paper, but the trends are a good indicator that this mechanism can be used to explain many of the experimental features.

Along with resistive restrike, which may explain additional channel formation, we also must explain the lack of additional channels formed in several of the “triggered” shots (Fig. 4).

The same physical process must occur, in that the plasma channels experience a rapid increase in resistivity, so we can also consider the effects of this on the collisionless skin depth  $\delta$ . This is given by  $\delta = \sqrt{\rho/\pi f \mu}$ , (where  $r$  is resistivity,  $f$  is frequency, and  $\mu$  is permeability) and increases as  $\rho^{1/2}$  and the current penetrates into the bulk of the solid liner as the resistivity increases. The high-electron density here ( $> 10^{22} \text{ cm}^{-3}$ ) can sustain much larger currents at low-drift velocity with minimal heating of the solid aluminum, and so the electron drift velocity can be lower than  $u_{\text{drift,critical}}$ . The load resistance remains low, and so does not drive a high-resistive voltage, and additional plasma channels are not required to carry the main current.

It is likely that both the restrike and skin depth processes occurs simultaneously. Which of the two processes dominates is simply a question of the precise plasma conditions as they develop and the timescale for each to have a significant effect. The result is that, in the experiments, both are seen. It seems that a resistivity increase due to the ion acoustic instability can reasonably well describe the main feature of the liner experiments at 1 MA. For this to be the dominant mechanism, the current must be carried in an initial surface plasma at least primarily. This is consistent with the experiments, but more detailed data and analysis of the initial and subsequent plasma formation are needed to be fully confident.

## V. CONCLUSION

A series of experimental studies was carried out on MagLIF-scale aluminum liners on the 1-MA COBRA device in which an azimuthal vacuum gap was introduced in the connection to the generator. Optical framing images denote the appearance and evolution of discrete current carrying plasma locations around the liner azimuth which have previously been directly linked to sustained nonuniformity of the current density in the liners using magnetic field probe arrays [2]. MHD simulations using the Gorgon code show that plasma breakdown of the vacuum gap leads to rapid uniformity of the current density for any gap size, in contrast to the experiments. This is likely to be a result of the need to set magnetic field boundary conditions close to the liner to drive the main current. However, the observed evolution of the plasma channels and currents density can be reasonably well explained by the development of increased resistivity in the plasma as the drive current increases. This limits the amount of current an individual plasma channels can carry, and either forces the formation of additional channels through resistive restrike of the vacuum gap or causes the current to flow in the liner bulk at later times through an increase in the electrical skin depth. Plasma evolution suggests both of these scenarios are observed experimentally. Estimates of the number of channels and the timescales of their formation are in reasonable agreement with the ion acoustic instability mechanism for the experimental plasma parameters.

## ACKNOWLEDGMENT

The authors would like to thank T. Blanchard and H. Wilhelm for supporting the experimental campaign on COBRA.

## REFERENCES

- [1] S. C. Bott-Suzuki *et al.*, "Investigation of the effect of a power feed vacuum gap in solid liner experiments at 1 MA," *Phys. Plasmas*, vol. 22, no. 9, p. 094501, 2015.
- [2] S. C. Bott-Suzuki *et al.*, "Study of the time-resolved, 3-dimensional current density distribution in solid metallic liners at 1 MA," *Phys. Plasmas*, vol. 23, no. 9, p. 092711, 2016.
- [3] W. A. Stygar *et al.*, "Architecture of petawatt-class z-pinch accelerators," *Phys. Rev. ST Accel. Beams*, vol. 10, no. 3, p. 030401, 2007.
- [4] C. L. Olson, "9 inertial confinement fusion: z-pinch," in *Nuclear Energy (Landolt-Börnstein—Group VIII Advanced Materials and Technologies)*, vol. 3B. Berlin, Germany: Springer-Verlag, 2005, pp. 495–528, ch. 9.
- [5] S. A. Slutz *et al.*, "Pulsed-power-driven cylindrical liner implosions of laser preheated fuel magnetized with an axial field," *Phys. Plasmas*, vol. 17, no. 5, p. 056303, 2010.
- [6] T. J. Awe *et al.*, "Observations of modified three-dimensional instability structure for imploding z-pinch liners that are premagnetized with an axial field," *Phys. Rev. Lett.*, vol. 111, no. 23, p. 235005, 2013.
- [7] M. R. Gomez *et al.*, "Demonstration of thermonuclear conditions in magnetized liner inertial fusion experiments," *Phys. Plasmas*, vol. 22, no. 5, p. 056306, 2015.
- [8] R. D. McBride *et al.*, "Beryllium liner implosion experiments on the Z accelerator in preparation for magnetized liner inertial fusion," *Phys. Plasmas*, vol. 20, no. 5, p. 056309, 2013.
- [9] J. B. Greenly, J. D. Douglas, D. A. Hammer, B. R. Kusse, S. C. Glidden, and H. D. Sanders, "A IMA, variable risetime pulse generator for high energy density plasma research," *Rev. Sci. Instrum.*, vol. 79, no. 7, p. 073501, 2008.
- [10] S. W. Cordaro *et al.*, "Two dimensional triangulation of breakdown in a high voltage coaxial gap," *Rev. Sci. Instrum.*, vol. 86, no. 7, p. 073503, 2015.
- [11] J. P. Chittenden, S. V. Lebedev, C. A. Jennings, S. N. Bland, and A. Ciardi, "X-ray generation mechanisms in three-dimensional simulations of wire array Z-pinches," *Plasma Phys. Controlled Fusion*, vol. 46, no. 12B, pp. B457–B476, 2004.
- [12] D. D. Ryutov, M. S. Derzon, M. K. Matzen, "The physics of fast Z pinches," *Rev. Mod. Phys.*, vol. 72, no. 1, p. 167, 2000.
- [13] S. V. Lebedev, D. A. Hammer, M. E. Cuneo, and D. B. Sinars, "Effect of trailing mass on scaling of X-ray power in wire array Z-pinches," in *Proc. AIP Conf.*, vol. 808, 2006, p. 73.



**Simon C. Bott-Suzuki** (M'07) received the M.Phys. degree in chemical physics and the Ph.D. degree in physics from Sheffield University, Sheffield, U.K., in 1999 and 2004, respectively.

He subsequently carried out post-doctoral research with Imperial College London, London, U.K. He was with the University of California San Diego, San Diego, CA, USA, in 2006. He is currently an Assistant Research Scientist with the Center for Energy Research, UC San Diego, and a Visiting Assistant Professor with Cornell University, Ithaca, NY, USA. He is involved in the experimental analysis of plasmas generated using pulsed-power techniques and their application in inertial fusion, basic plasma physics, and laboratory astrophysics. He has authored over 60 journal papers.

Dr. Bott-Suzuki has served as the Co-Chair for the 9th International Conference on Dense Z-Pinches (Napa, CA 2014). He has also served in various roles for the ICOPS conference series and as a Guest Editor for the Fourth and Fifth Special Issues on Z-pinch plasmas published in the IEEE TRANSACTIONS ON PLASMA SCIENCE.



**Samuel W. Cordaro** received the B.S. degree in applied physics from the Rensselaer Polytechnic Institute, Troy, NY, in 2013. He is currently pursuing the Ph.D. degree with the University of California San Diego, San Diego, CA, USA, where he focused on the current density distribution through pulsed-power liners.

**L. Atoyán** (GS'13), photograph and biography not available at the time of publication.

**T. Byvank** (GS'14), photograph and biography not available at the time of publication.

**W. Potter**, photograph and biography not available at the time of publication.

**B. R. Kusse** photograph and biography not available at the time of publication.

**J. B. Greenly** photograph and biography not available at the time of publication.

**D. A. Hammer** (F'95), photograph and biography not available at the time of publication.

**C. A. Jennings**, photograph and biography not available at the time of publication.